Journal Pre-proof

Recovery of immunoglobulin G from rabbit serum using κ-carrageenan-modified hybrid magnetic nanoparticles

Flávia F. Magalhães, Mafalda R. Almeida, Sofia F. Soares, Tito Trindade, Mara G. Freire, Ana Luísa Daniel-da-Silva, Ana P.M. Tavares

Please cite this article as: F.F. Magalhães, M.R. Almeida, S.F. Soares, et al., Recovery of immunoglobulin G from rabbit serum using κ-carrageenan-modified hybrid magnetic nanoparticles, *International Journal of Biological Macromolecules*(2018), https://doi.org/10.1016/j.ijbiomac.2020.02.135

This is a PDF file of an article that has undergone enhancements after acceptance, such as the addition of a cover page and metadata, and formatting for readability, but it is not yet the definitive version of record. This version will undergo additional copyediting, typesetting and review before it is published in its final form, but we are providing this version to give early visibility of the article. Please note that, during the production process, errors may be discovered which could affect the content, and all legal disclaimers that apply to the journal pertain.

Recovery of immunoglobulin G from rabbit serum using κ-carrageenan-modified hybrid magnetic nanoparticles

Flávia F. Magalhães[†], Mafalda R. Almeida[†], Sofia F. Soares, Tito Trindade, Mara G. Freire, Ana Luísa Daniel-da-Silva, Ana P. M. Tavares*

CICECO – Aveiro Institute of Materials, Department of Chemistry, University of Aveiro, 3810-193 Aveiro, Portugal

[†]These authors contributed equally to this work.

*Corresponding author

E-mail address: aptavares@ua.pt

Abstract

Immunoglobulin G (IgG) has been used in the treatment of cancer, autoimmune diseases and neurological disorders, however, the current technologies to purify and recover IgG from biological media are of high-cost and time-consuming, resulting in high-cost products. In this sense, the search for cost-effective technologies to obtain highly pure and active IgG is highly required. The present work proposes a simple and efficient method for the purification and recovery of IgG from rabbit serum using magnetic iron oxide nanoparticles (magnetite, Fe_3O_4) coated with hybrid shells of a siliceous material modified with the anionic polysaccharide κ-carrageenan. Experimental parameters such as pH, contact time between the hybrid magnetic nanoparticles (HMNPs) and rabbit serum, and total protein concentration or dilution factor of serum were evaluated. The best results were achieved at pH 5.0, with a contact time of 60 min and using a rabbit serum with a total protein concentration of 4.8 mg.mL^{-1}. Under these conditions, it was obtained an IgG purification factor and adsorption yield onto the HMNPs of 3.0 and 90%, respectively. The desorption of IgG from the HMNPs was evaluated using two strategies: a KCl aqueous solution and buffered aqueous solutions. Comparing to the initial rabbit serum, an IgG purification factor of 2.7 with a recovery yield of 74% were obtained using a buffered aqueous solution at pH 7.0. After desorption, the secondary structure of IgG and other proteins was evaluated by circular dichroism and no changes in the secondary structure were observed, meaning that the IgG integrity is kept after the adsorption and desorption steps. In summary, the application of HMNPs in the purification of IgG from serum samples has a high potential as a new downstream platform.

Keywords: Immunoglobulin G; Adsorption; κ-Carrageenan; Magnetic nanoparticles; Recovery.

1. Introduction

During the last two decades, the field of new drugs development has moved its focus from small-molecule compounds to large-molecule proteins and other biopharmaceuticals [1]. Biopharmaceuticals have significantly improved the treatment of many diseases and sometimes are the only approved therapies available for a specific disease. These biological-based products, which include antibodies, recombinant proteins, and nucleic-acid-based products, have applications in several therapeutic areas [2]. Particularly, antibodies such as Immunoglobulin G (IgG) have been used in the treatment of cancer, as transporters of toxins or radiolabelled isotopes to cancerous cells, and in the treatment of autoimmune diseases and neurological disorders [3]. To these ends, the production of IgG for therapeutic applications must meet high efficiency and safety standards, demanding high quality and high purity IgG [4]. However, the currently used downstream technologies (mainly chromatographic techniques - ion exchange, gel permeation and affinity chromatography) for the IgG purification are highly expensive and require extra steps for the efficient removal of impurities [5]. Therefore, there is a high demand for the development of cost-effective techniques to obtain highly pure IgG from the original complex matrices without loss of its stability and biological activity. In order to suppress these and other shortcomings related to traditional methods, the extraction and purification of IgG using novel technologies must be investigated. The extraction of IgG has been studied using liquid-liquid systems, predominantly aqueous biphasic systems [3−6]. For instance, Mondal *et al*. [3] investigated the purification of rabbit serum IgG using ionic-liquid-based aqueous biphasic systems. Besides liquid-liquid systems, solid-liquid systems comprising magnetic nanoparticles (MNPs) as novel adsorbents have also been explored [7−12]. For example, Bereli *et al.* [7] conducted a study on the purification of IgG using

magnetic nanoparticles based on acrylate functionalized with methyl ester N-methacryloyl-(L)-histidine.

The main interest in MNPs is due to their particular properties combining the merits of rapid magnetic separation with a high surface area. The small size, typically below 100 nm, endows MNPs with a high specific surface area that favours the adsorption process. Iron oxide nanoparticles [13], such as those of ferrimagnetic magnetite (Fe_3O_4), feature a magnetically separable ability which is highly advantageous for an easy and fast magnetic separation of the material from the surrounding medium [13]. MNPs have potential in several fields, such as in the food sector [13], transport and drug delivery [14], separation and purification of enzymes and proteins [15–17], environmental remediation [18] and biomedical and biological applications [19].

The short separation time, scalability, and easy automation make the MNPs application advantageous in separation fields [13]. However, the pH and ionic strength conditions which might be required for the stability of the biological molecules can degrade the nanoparticles, for example by oxidation processes [20]. To avoid this phenomenon, MNPs can be surface modified through chemical functionalization or by encapsulation within shells of other materials [15]. The shells encapsulation can be performed in order to increase the nanoparticle's chemical and colloidal stability and ascribes adequate surface functionality for the desired effect. Essentially, the encapsulated MNPs should display high affinity to the target biomolecules allowing their subsequent separation from the complex medium by applying a magnet. Moreover, biopolymers can establish interactions with biomolecules via hydrophobic and/or electrostatic interactions [21], which could be used to tailor the separation performance. Since many biopolymers are polyelectrolytes, it is possible to employ these compounds in the encapsulation of magnetic nanoparticles to provide affinity towards target biomolecules such as IgG

4

[22]. In this way, MNPs surface modified with biopolymers are promising for the adsorption of biomolecules because they combine the magnetic properties of the core with specific chemical functionalities of the biopolymeric outer-shells [23].

Soares et al. [23] have developed core@shell type magnetic nanoparticles comprising a magnetic core encapsulated with a shell of an organic-inorganic hybrid material highly enriched in polysaccharides. These hybrid shells exhibit flexibility and reactivity from the polymer functional groups and a chemically robust coating due to the inorganic component (silica), thus creating improved properties when compared with the individual components. The application of these hybrid materials has been of great interest due to their biocompatibility properties, low cost and wide availability of biopolymers, such as κ-carrageenan (κ-CRG) [23, 24]. Therefore, HMNPs have high potential as new nanosorbents for the purification and recovery of IgG, which is described in this work for the first time.

2. Experimental

2.1. Materials

Tetraethylorthosilicate (TEOS) [$Si(OC_2H_5)_4$, > 99.0%], κ-carrageenan (κ-CRG), 3-(triethoxysilyl)propyl isocyanate (ICPTES) [$(C_2H_5O)_3Si(CH_2)_3NCO$, 95.0%], ferrous sulfate heptahydrate ($FeSO_4.7H_2O$, > 99.0%), sodium phosphate dibasic heptahydrate ($Na_2HPO_4.7H_2O$, > 98%) and rabbit serum (total protein concentration between 40-70 mg.mL^{-1}) were obtained from Sigma-Aldrich. N-dimethylformamide (DMF) [$HCON(CH_3)_2$, > 99.0%] and ethanol (CH_3CH_2OH) were purchased from Carlo Erba. Ammonia solution (25% NH_3), methanol (CH_3OH) and sodium carbonate (Na_2CO_3, > 99.9%) were obtained from VWR Chemicals Prolabo. Potassium nitrate (KNO_3, > 97.2% (m/m)), sodium hydrogen carbonate ($NaHCO_3$ > 99%) and potassium hydroxide

5

(KOH) were acquired from Labchem. Potassium chloride (KCl) and citric acid ($C_6H_8O_7.H_2O$) were supplied by Chem-Lab and Panreac, respectively. All solutions were prepared with Milli-Q water obtained from Synergy equipment from Millipore with a 0.22 μm filter.

2.2. Synthesis of hybrid magnetic nanoparticles

Hybrid magnetic nanoparticles (HMNPs) were synthesized as previously described [25]. The magnetite (Fe_3O_4) core was synthesized by oxidative hydrolysis of $FeSO_4.7H_2O$ under a nitrogen stream, according to the methodology described by Oliveira-Silva et al. [26]. The synthesis of the alkoxysilane derivative of κ-carrageenan (SiCRG) was carried out in an inert and dry atmosphere of N_2 using an aprotic solvent (DMF), allowing the reaction between the biopolymer κ-CRG and the isocyanate groups of ICPTES. The encapsulation of the magnetite nanoparticles within shells of a hybrid material comprising silica and κ-CRG was possible through the base-catalysed hydrolysis and condensation of a mixture of TEOS and Si-CRG performed in the presence of the magnetite nanoparticles, as previously described by Soares et al. [18].

2.3. Hybrid magnetic nanoparticles characterization

The powder X-ray diffractogram of HMNPs was recorded between 10 and 65 ° (2θ) in a Rigaku Geigerflex Dmax-C diffractometer (Rigaku, Tokyo, Japan) equipped with a CuKα monochromatic radiation source, with a step size of 0.026º and time per step of 350 s. The Fourier transform infrared (FTIR) spectra of the materials were acquired in a Bruker Optics Tensor 27 spectrometer (Bruker, Billerica, MA, USA) employing a horizontal cell of attenuated total reflectance (ATR), with a total of 256 scans in the range of 350 to 4000 cm^{-1} with a resolution of 4 cm^{-1}. Elemental analysis of carbon,

nitrogen, and hydrogen was obtained on the Leco Truspec-Micro CHNS 630-200-200 equipment (Saint Joseph, MI, USA). The specific surface area and pore volume were examined by N_2 sorption isotherms using a Gemini V-2380 surface area analyser (Micromeritics, Norcross, GA, USA). Prior to the measurements, the samples were degassed overnight at 80 ℃. The pore volume (V_p) was determined by BJH (Barrett-Joyner-Halenda) model and the specific surface area (S_{BET}) was determined by the Brunaer–Emmett–Teller (BET) equation with multipoint adsorption isotherms of N_2 at -196 ℃. The surface charge of HMNPs was determined by zeta potential measurements through electrophoretic light scattering, performed using a Zetasizer Nano ZS instrument equipped with a HeNe laser operating at 633 nm and a scattering detector at 173º, from Malvern Instruments (Malvern, UK). The samples were pre-diluted in Milli-Q water, the pH adjusted with NaOH (0.01 M) and HCl (0.01 M) solution to obtain pH solutions ranging from 3.5 to 9.5, and three readings were taken for each sample. The morphology and size of the HMNPs were assessed by transmission electron microscopy (TEM) using the Hitachi H-9000 TEM microscope (Hitachi, Tokyo, Japan), operating at 300 kV and the high-resolution TEM microscope JEOL 2200FS (Jeol, Tokyo, Japan), operating at 200 kV. Samples for analysis were prepared by deposition of HMNP suspensions in ethanol on a copper grid coated with an amorphous carbon film. Subsequently, the samples were subjected to evaporation of the solvent. The particle size was calculated by analyzing TEM images with the software Image J.

2.4. Adsorption and purification of IgG from rabbit serum

The adsorption and purification of IgG from rabbit serum using HMNPs were investigated in a batch system. Several parameters were optimized in order to maximize the IgG adsorption in terms of adsorption yield and purity, namely pH, protein

concentration or serum dilution and contact time. The HMNPs were washed and then 2.0 (±0.1) mg were added to an aqueous solution of rabbit serum in an orbital shaking. Subsequently, the HMNPs were magnetically separated from the aqueous solution (supernatant), as schematized in Fig. S1 in the Supporting Information.

The pH effect on the IgG adsorption and purification was studied using citrate-phosphate buffer at pH values of 3.0, 4.0 and 5.0; phosphate buffer at pH values of 6.0, 7.0 and 8.0; and carbonate buffer at pH 9.0. 100 μL of buffer and 100 μL of water diluted rabbit serum with 0.6 mg.mL^{-1} of total protein were added to the HMNPs. This mixture was stirred for 60 min in an orbital shaker. A control was prepared using 50 μL of diluted rabbit serum (0.6 mg.mL^{-1} of total protein content) and 50 μL of distilled water. The influence of the contact time between the rabbit serum and the HMNPs was also investigated. The experiments were performed by adding 100 μL of citrate-phosphate buffer at pH 5.0 and 100 μL of water diluted rabbit serum (0.6 mg.mL^{-1} of total protein content) to the HMNPs. The mixture was stirred during periods between 15 and 90 min in an orbital shaker. A control was prepared with 50 μL of water diluted rabbit serum (0.6 mg.mL^{-1} of total protein) and 50 μL of citrate-phosphate buffer at pH 5.0. Finally, the effect of serum dilution was also evaluated by adding 100 μL of citrate-phosphate buffer at pH 5.0 and 100 μL of rabbit serum diluted at different concentrations: from 0.3 mg.mL^{-1} to 4.8 mg.mL^{-1}. The mixture was stirred for 60 min in an orbital shaker. A control was prepared with 50 μL of rabbit serum of each dilution and 50 μL of distilled water. At least three individual experiments were carried out for each condition, allowing the determination of the average recovery yield and purification factor and respective standard deviations.

The rabbit serum, supernatant proteins, before and after IgG adsorption, were quantified by size-exclusion high-performance liquid chromatography (SE-HPLC) (Chromaster,

VWR Hitachi) with a Shodex Protein KW-802.5 (8mm x 300mm) column. Before injection, the samples were diluted 10 times with the mobile phase (100 mM phosphate buffer + NaCl 0.3 M). The mobile phase was run isocratically at 0.5 mL.min^{-1}. The column oven and autosampler were kept at 40 °C and 10 °C, respectively. The injection volume was 25 μL. The wavelength was set at 280 nm using a DAD detector. The chromatograms were analyzed using the OriginPro software. The IgG purity factor and adsorption yield were determined according to equations 1 and 2. The purification factor of IgG (PF_{IgG}) onto the HMNPs (adsorbed IgG) was calculated according to Equation 1:

$$PF_{IgG} = \frac{\%Purity_{IgG\ adsorbed}}{\%Purity_{IgG\ initial}} \qquad (1)$$

where %Purity$_{IgG\ adsorbed}$ and %Purity$_{IgG\ initial}$ correspond to the purity level of IgG adsorbed onto the HMNPs and the purity level of IgG in the rabbit serum samples, respectively.

The adsorption yield (%Yield$_{IgG}$) of IgG onto the material was calculated according to equation (2):

$$\%Yield_{IgG} = \frac{[IgG]_{adsorbed}}{[IgG]_{initial}} \times 100 \qquad (2)$$

where [IgG]$_{adsorbed}$ and [IgG]$_{initial}$ correspond to the IgG concentration onto the HMNPs and the initial concentration of IgG in the rabbit serum taking into account all dilutions carried out, respectively.

2.5. Desorption of IgG from hybrid magnetic nanoparticles

In all experiments, firstly IgG was adsorbed onto 2 mg of HMNPs (IgG@HMNP) at pH 5.0, 60 min of contact and rabbit serum with a total protein's concentration of 4.8 mg.mL^{-1}. Then, the IgG desorption was performed by applying two distinct methods. In the first method, 200 μL of a KCl aqueous solution of variable concentration (0.10 M; 0.25 M; 0.5 M) was added to IgG@HMNP and stirred for 60 min in an orbital shaker. The contact time was also evaluated for 60 and 120 min using 200 μL of KCl 0.5 M. Finally, the ratio of IgG@HMNP mass (mg) and KCl solution (μL) 0.5 M of 1:100 and 1:200 was evaluated for 60 min of contact time. In the second method, the pH effect was investigated using buffered aqueous solutions. 400 μL of phosphate buffer 50 mM at pH 7.0 or 8.0, or carbonate buffer 50 mM at pH 9.0 or 10.0 were added to IgG@HMNP. The mixture was stirred for 60 min using an orbital shaker. At least three individual experiments were carried out for each condition, allowing the determination of the average recovery yield and purification factor and respective standard deviations. The desorbed IgG was quantified by SE-HPLC as described above.

The purification factor of IgG (DPF$_{IgG}$) after the desorption from the HMNPs was calculated according to Equation 3:

$$DPF_{IgG} = \frac{\%Purity_{IgG\ desorbed}}{\%Purity_{IgG\ initial}} \qquad (3)$$

where %Purity$_{IgG\ desorbed}$ and %Purity$_{IgG\ initial}$ correspond to the purity level of IgG desorbed and the purity level of IgG in the rabbit serum sample, respectively.

The recovery yield (%DYield$_{IgG}$) of desorbed IgG from the HMNPs was calculated according to equation (4):

$$\%DYield_{IgG} = \frac{[IgG]_{desorbed}}{[IgG]_{initial}} \times 100 \qquad (4)$$

10

where $[IgG]_{desorbed}$ and $[IgG]_{initial}$ correspond to the desorbed IgG concentration and the initial concentration of IgG in the rabbit serum, respectively.

2.7. Evaluation of the IgG secondary structure by circular dichroism

The IgG secondary structure after the desorption step was evaluated by circular dichroism (CD) using a Jasco J-1500 CD spectrometer. CD spectra were recorded from 200 to 260 nm using quartz circular dichroism cuvettes (0.1 cm) at room temperature (ca. 25ºC). Each CD spectrum is the result of four accumulations recorded in millidegrees. The following acquisition parameters were used: data pitch, 0.5 nm; bandwidth, 1.0 nm; response, 1 s; and scan speed, 50 nm.min^{-1}.

3. Results and Discussion

3.1. Characterization of hybrid magnetic nanoparticles

The magnetic cores once synthesized have been encapsulated by organic-inorganic hybrid shells to produce core/shell particles as illustrated in Fig. 1. The resulting HMNP were then characterized through their chemical composition, size, surface area, porosity, and surface charge.
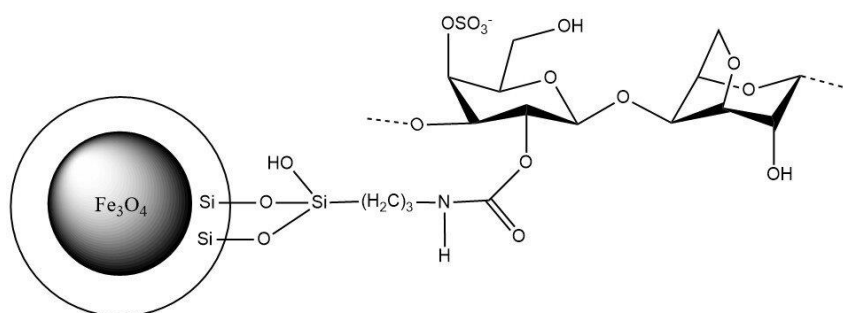

Fig. 1. Scheme of hybrid magnetic nanoparticles used for the IgG adsorption and purification from rabbit serum.

Fig. 2 (a) shows the powder X-ray diffractogram of the magnetite powders used as cores, along with the labeling of the respective Miller indices. The diffraction peaks at 18.4^{o} (111), 30.2^{o} (220), 35.5^{o} (311), 43.1^{o} (400), 53.6^{o} (422), 57.1^{o} (511) and 62.7^{o} (440) are consistent with the presence of magnetite with cubic inverse spinel structure (ICDDPDF nº 04-006-6550). Similar XRD patterns were observed for the HMNP (Fig. 2 (b)), confirming that the cores in the hybrid nanoparticles are magnetite [27, 28]. Fig. 2 (b) also shows a broad background signal and a diffuse peak at about 21º theta, characteristic of short-range order in amorphous silica and supporting the presence of the hybrid siliceous shells surrounding the magnetic cores.
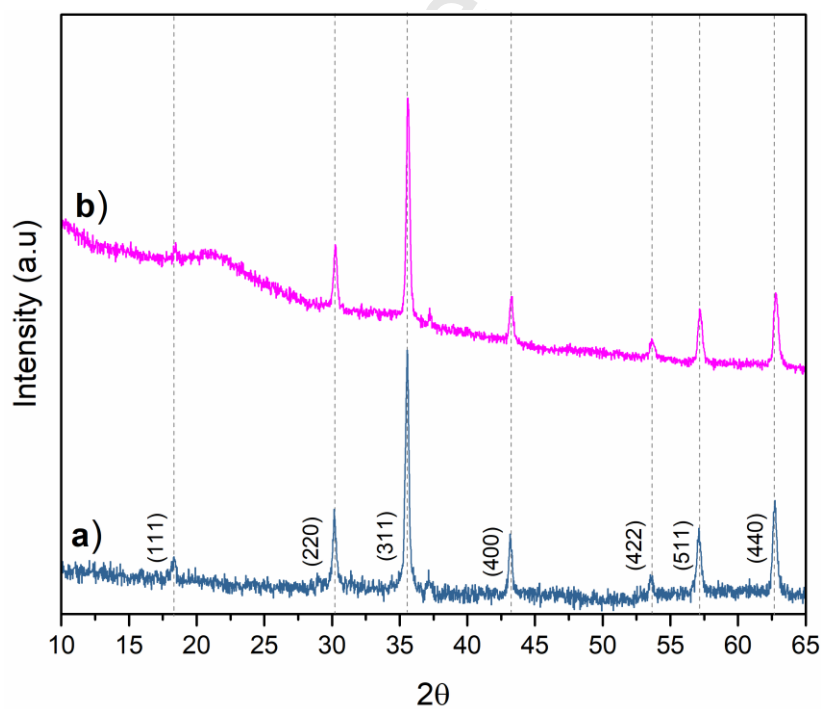

Fig. 2. Powder X-ray diffractogram patterns of Fe_3O_4 (a) and HMNP (b) nanoparticles.

The κ-CRG, SiCRG, HMNP and Fe_3O_4 samples were analyzed by infrared spectroscopy, whose results and detailed identification of the diagnosis vibrational bands are included in the Fig. S2 (Supporting Information) providing evidence of the

organic-inorganic hybrid nature of the HMNPs. Briefly, in the HMNP spectrum (Fig S2 (c)) the encapsulation of the magnetite core is confirmed by the appearance of new vibrational bands characteristic of silica (436 cm^{-1} ascribed to O–Si–O vibration) and of the biopolymer κ-carrageenan (843 cm^{-1} due to C-O-S vibration, 1045 cm^{-1} due to C-O and C-OH vibrations, 1220 cm^{-1} owing to S-O asymmetric stretching in the –OSO$_3^-$ groups) [18]. These bands confirm the presence of a siliceous material containing κ-carrageenan coating the magnetic cores.

The elemental analysis confirmed the functionalization of the HMNPs through the comparison of carbon and sulfur contents in the particles, before and after the encapsulation with the hybrid shell. The results indicate that the magnetic core (Fe$_3$O$_4$) contains 0.068 (± 0.006) wt% of carbon, 0.162 (± 0.042) wt% of hydrogen, 0.012 (± 0.004) wt% of nitrogen, and no sulfur content was detected. Since the magnetic core is composed of the crystalline phase of Fe$_3$O$_4$, it is expected to have low carbon, nitrogen and sulfur contents. The HMNPs contain 23.4 (± 0.3) wt% of carbon, 4.40 (± 0.22) wt% of hydrogen, 0.299 (± 0.014) wt% of nitrogen and 5.85 (± 0.29) wt% of sulfur. It is worth noting that after encapsulation the contents in carbon, nitrogen, and sulfur markedly increased, which is in agreement with the formation of a shell with organic-inorganic hybrid nature, highly enriched in the biopolymer κ-carrageenan, around the magnetic cores.

Fig. 3 shows the TEM images of the magnetic core (Fe$_3$O$_4$) (Fig. 3 (a)) and the HMNP (Fig. 3 (b)). The HMNPs have a nearly spherical shape, comprising the magnetite core (darker zone) coated with the hybrid shells (lighter zone), thus confirming that the encapsulation of the MNP was successful. The average size of the magnetic core was found to be 48.9 (± 5.9) nm and, after surface modification, the coating thickness was 20.7 (± 2.3) nm.
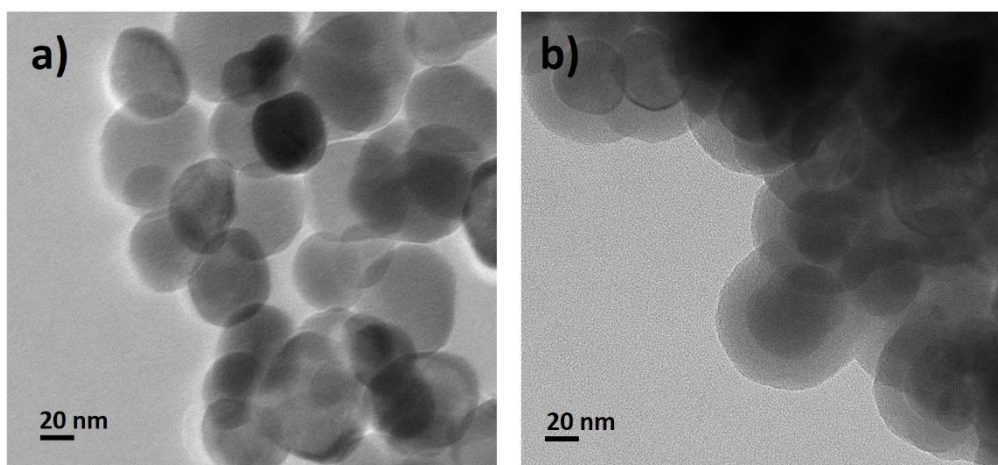
Fig. 3. TEM images of Fe_3O_4 (a) and HMNP (b).

The specific surface area (S_{BET}) and pore volume of the synthesized HMNPs were obtained by nitrogen-sorption measurements. The MNPs have a S_{BET} of 23.8 m²/g and a pore volume of 0.080 cm³/g. After encapsulation, HMNPs have a S_{BET} of 6.9 m²/g and a pore volume of 0.011 cm³/g. These values show a decrease in the specific surface area after the encapsulation that can be due to an increase of the diameter of the particles after the encapsulation, with HMNPs showing a high S_{BET}.

Zeta potential measurements allowed to estimate the surface charge and to get information about colloidal stability. The zeta potential values were smaller than -25mV in the pH range investigated, from pH 3.5 to 8.5 (as shown in Fig. S3 in the Supporting Information). The negative surface charge of HMNP is consistent with the presence of the anionic sulfonate groups of κ-carrageenan over the surface of the material and the highly negative zeta potential accounts for the colloidal stability due to electrostatic repulsion [19].

3.2 Adsorption and purification of IgG from rabbit serum

14

The synthesized HMNPs were ascertained in what concerns their capacity to adsorb and purify IgG from rabbit serum. Several parameters were studied in order to maximize the IgG adsorption yield and the purification factor, namely pH, contact time and serum dilution or protein content. Firstly, the pH effect in the IgG adsorption onto HMNPs was studied at distinct pH values (pH range between 3.0 and 9.0). The rabbit serum with a protein concentration of 0.6 mg.mL^{-1} and a contact time of 60 min was maintained constant during all these assays. The results of IgG adsorption yield and purification factor on the material are depicted in Fig. 4 (A). At pH 3.0 and 4.0, it was not detected any peak on the SE-HPLC chromatograms, which is probably due to the total proteins denaturation, which is a common feature for proteins at very acidic pH values [29]. Comparing the results for higher pH values, it is possible to observe a decrease of the IgG purification factor and adsorption yield with the increase of pH. The best results were attained at pH 5.0, with an IgG purification factor of 1.3 times and an IgG adsorption yield of 93%. At pH 5.0, the IgG has a positive total charge (rabbit IgG pI of 7.8 [4]), while the albumin (main impurity of rabbit serum) is closer to its pI (albumin pI of 5.65 [30]). On the other hand, according to the previous zeta potential analysis, HMNPs have a negative surface charge. Thus, the higher IgG purity and yield levels at lower pH values can be explained by electrostatic interactions occurring between the positively charged IgG and the negative charged sulphate groups from κ-CRG [31, 32]. This increase in the purity of IgG in the material means that more impurities (other proteins) remain in the supernatant and are not completely adsorbed onto the material. On the other hand, the IgG adsorption profile at pH 6.0 and 7.0 show the opposite behavior. Although at these pH values the IgG and albumin are positively and negatively charged, respectively, the IgG purity and adsorption yield decrease when compared to the results obtained at pH 5.0. This fact is due to the proximity to the pI of

IgG to these values and still significant content of IgG not totally positively charged. Thus, pH 5.0 was selected for the next experiments.

The effect of the contact time between the rabbit serum and the HMNPs was studied using the same proteins concentration in serum (0.6 mg.mL^{-1}) of the previous assays. Since the main interest is to obtain IgG with high purity level and to develop a process of low cost, the contact time is an important parameter to evaluate. Eight contact times, between 15 and 90 min, were evaluated. The results presented in Fig. 4 (B) reveal that the contact time has a significant effect on the IgG adsorption yield and purification factor. After 30 min of contact time, the highest IgG purification factor of 3.7 was obtained, but an IgG adsorption yield of 54% is attained. These results reveal that after 30 min of contact, less albumin is adsorbed onto HMNPs leading to an increase in the IgG purity. On the other hand, the IgG adsorption yield reaches the maximum at 60 min, with a value of 93%, but the purification factor decreases to 1.3 due to an increase of adsorbed impurities or other proteins. After longer periods of time (90 min), the IgG purity and yield decreased, probably due to their replacement by albumin as the main impurity present in serum.

The rabbit serum dilution was finally investigated at the optimized pH and contact time (pH 5.0 and 60 min). These parameters were selected considering the best IgG adsorption yield. Seven dilutions were studied with a final total protein concentration ranging between 0.3 and 4.8 mg.mL^{-1}. The results obtained are presented in Fig. 4 (C). Regarding the IgG purity, a concentration of proteins of 4.8 mg.mL^{-1} leads to a maximum purification factor of IgG of 3.0. Overall, by increasing the total concentration of proteins it is possible to increase the IgG purity adsorbed in the material. On the other hand, IgG adsorption yields higher than 90% were observed for all concentrations studied, with a value of 100% when serum with protein

16

concentrations of 1.0 and 0.8 mg.mL^{-1} were used. In fact, the contact time between the rabbit serum and the HMNP of 60 min ensures high yields, being in agreement with the previous results shown in Fig. 4 (B).

Taking into account the optimized conditions for IgG purity and adsorption yield, namely the following conditions: pH 5.0, 60 min of contact and proteins concentration in serum of 4.8 mg.mL^{-1}, it is possible to obtain IgG with a purification factor of 3.0 (purity level of 60%) and an adsorption yield of 90%.

In order to evaluate the presence of adsorbed proteins onto the HMNPs, ATR-FTIR analysis of the samples was carried out (Fig. S4 in the Supporting Information). Proteins have a secondary structure formed by the interaction of their constituent amino acids. These structures are α-helix, β-sheet, β-turn, among others [3]. These structures produce a spectrum band between 1600 and 1690 cm^{-1} corresponding to the amide region I [3]. Within this range, the band related to β-sheet produces a characteristic band at 1635 cm^{-1}, the α-helix structure at 1660 cm^{-1} and the β-turn at 1645 cm^{-1} [3]. Comparing the two spectra given in Fig. S4, Supporting Information, it is clearly noticed the appearance of a new band near 1630 cm^{-1} in the HMNPs after the IgG adsorption, although a residual contribution of the water deformation vibration band is seen at 1640 cm^{-1} [3], thus confirming the presence of proteins in the HMNPs.

Hou et al. [8] investigated the IgG monoclonal antibody purification using modified $Fe_3O_4@SiO_2$ MNPs with protein A, which was covalently immobilized. These MNPs showed a good binding capacity for the chimeric anti-EGFR monoclonal antibody providing a purity of about 95% [8]. Salimi et al. [11] also proposed protein A carrying magnetic, monodisperse SiO_2 microspheres [Mag(SiO_2)], as an affinity sorbent for IgG purification from rabbit serum. By using protein A attached-Mag(SiO_2) microspheres an IgG purity higher than 95% was attained. Although the IgG purity described in these

17

reports is higher than in the present work, the use of protein A, one of the most expensive ligands used in monoclonal antibody purification, will significantly increase the overall processes cost, making them less attractive. In another material´s approach, Bereli et al. [7] studied the purification of IgG using methyl N-methacryloyl (L)-histidine ester functionalized acrylate-based MNPs, obtaining a purity of the eluted IgG of 85% with a yield about 78% [7]. However, in the present work, higher IgG adsorption yields were attained, higher than 90%, and reaching 100% when serum concentrations of 1.0 and 0.8 mg.mL^{-1} were used (Fig. 4). Comparing to our work, Bereli et al. [7] reported a material saturation when the protein concentration was higher than 1.0 mg/mL^{-1}. The opposite capacity of adsorption is obtained in the present work, being the best results achieved when higher concentrations of rabbit serum are used, namely 4.8 mg.mL^{-1}, leading to a maximum purification factor of IgG of 3.0.
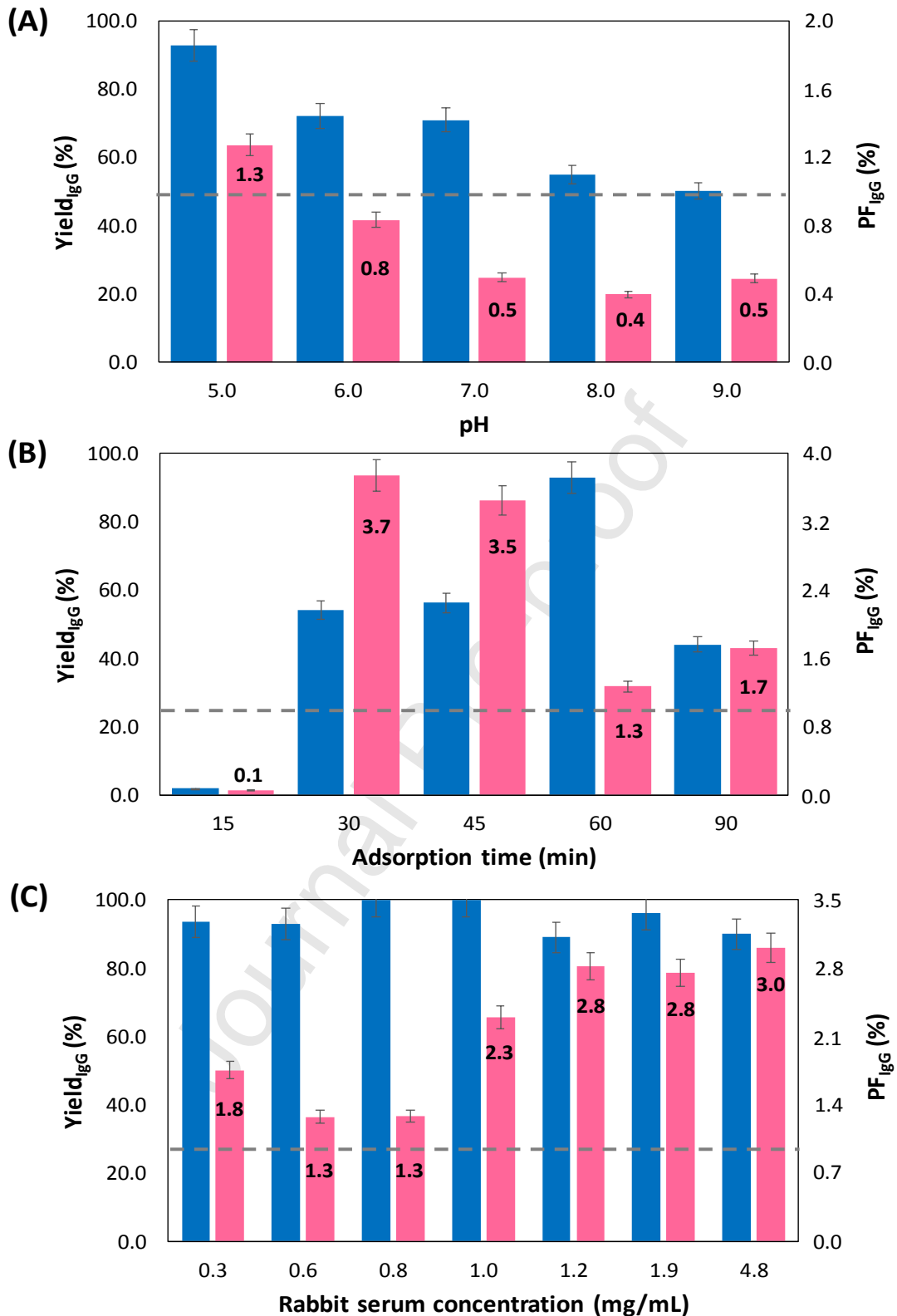
Fig. 4. Recovery yields (%Yield$_{IgG}$ – ■) and purification factors (PF$_{IgG}$ – ■) of IgG in HMNPs. The dashed line corresponds to the initial IgG purity in the rabbit serum (PF=1.0). (A) pH effect on the IgG adsorption and purification using 60 min of contact

time and a rabbit serum concentration of 0.6 mg.mL^{-1}. (B) Influence of the contact time between the rabbit serum and the HMNPs on the IgG adsorption and purification using citrate-phosphate buffer at pH 5.0 and a rabbit serum concentration of 0.6 mg.mL^{-1}. (C) Effect of rabbit serum concentration on the IgG adsorption and purification using citrate-phosphate buffer at pH 5.0 and 60 min of contact time.

3.3. Desorption of IgG from hybrid magnetic nanoparticles

This work intends to develop a process to purify IgG. Accordingly, after the selective adsorption of IgG, the target antibody needs to be recovered by desorption. In all desorption experiments, the IgG was firstly adsorbed at the optimized conditions (pH 5.0, 60 min of contact and proteins concentration in serum of 4.8 mg.mL^{-1}), as described above. To evaluate the IgG desorption effectiveness, the IgG recovery yield and purification factor were evaluated, before and after the IgG desorption by using two approaches: i) use of KCl aqueous solutions and ii) use of buffered solutions at four pH values (7.0, 8.0, 9.0 and 10.0). The effect of the KCl aqueous solution was addressed since κ-CRG has a high affinity for K$^+$ ions [33] and this salt has been already reported in other proteins desorption studies [34, 35]. According, it is expected that K$^+$ ions interact with the sulphate groups of the polysaccharide allowing the release of proteins from the material to the supernatant. For this purpose, three different parameters were evaluated: concentration of KCl, contact time and ratio of IgG@HMNP:KCl solution. Three concentrations of KCl aqueous solutions (0.25, 0.50 and 0.10 M) were investigated, maintaining constant the contact time (60 min) and the ratio IgG@HMNP:KCl solution (1:100). The results presented in Fig. 5 (A) indicate an increase in IgG purity with the increase of the KCl concentration, but still lower than the IgG purity in the rabbit serum, and an IgG recovery yield higher than 77%. The

contact time between the IgG@HMNP and the KCl solution also was evaluated using a 0.50 M KCl solution. Two different contact times, 60 and 120 min, with a 1:100 IgG@HMNP:KCl ratio were used. The results obtained (Fig. 5 (B)) reveal an increase in the IgG recovery yield from 78% to 97%. However, the IgG purification factor slightly decreased, from 1.4 to 1.2, after 120 min of contact time. Finally, the volume of KCl solution used for the IgG desorption was investigated. Two IgG@HMNP:KCl ratio were studied, namely 1:100 and 1:200, with a 0.5 M KCl solution and a contact time of 60 min. The results presented in Fig. 5 (C) indicate an IgG purification factor increase from 1.5 to 1.7 when higher volumes of KCl solution are used. Although several parameters were investigated to increase the IgG recovery yield and IgG purity, the purity values are always lower than those obtained in the previous assays, suggesting that K^+ ions are replacing all proteins without selectivity.
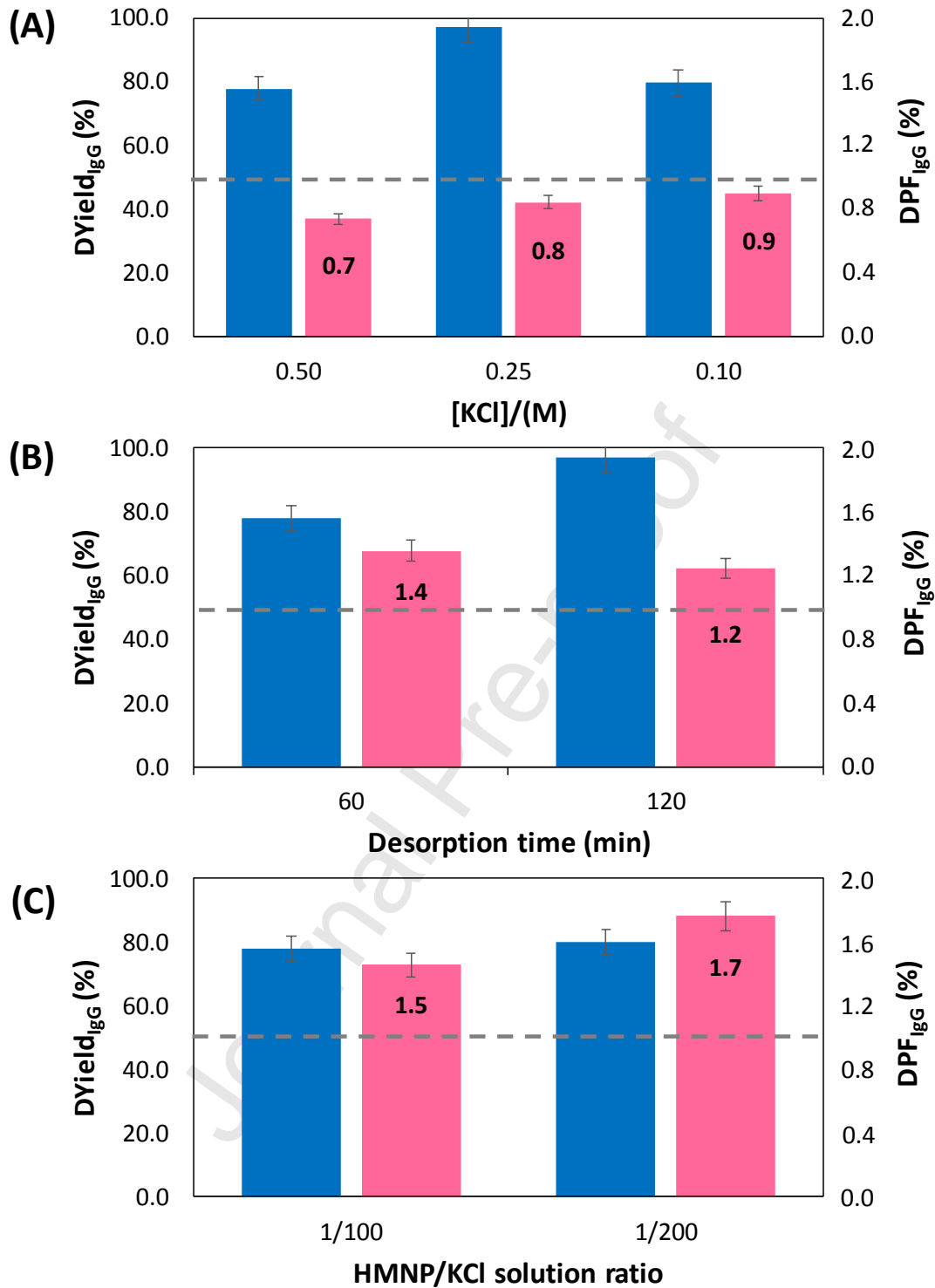
Fig. 5. Recovery yields (%DYield$_{IgG}$ – ■) and purification factors (DPF$_{IgG}$ – ■) of IgG desorbed from HMNPs using KCl. The dashed line corresponds to the initial IgG purity in the rabbit serum (PF = 1.0). (A) Effect of KCl aqueous solution on the IgG desorption using 60 min of contact time and 1/100 HMNP/KCl solution ratio. (B)

22

Influence of desorption time on the IgG desorption using 0.5 M KCl aqueous solution and 1/100 HMNP/KCl solution ratio. (C) Impact of IgG@HMNP mass (mg) and 0.5 M KCl solution (μL) ratio using 60 min of contact time.

Afterwards, the effect of the pH on the IgG desorption was studied at four pH values (7.0, 8.0, 9.0 and 10.0). This pH range was selected since the IgG adsorption is favored under acidic pH values, expecting that the use of buffered aqueous solutions with higher pH values will promote electrostatic repulsion between the HMNPs and IgG. The results presented in Fig. 6 show a significant decrease in the IgG recovery yield, from 74% to 24%, when higher pH values are used. This phenomenon can be related to the formation of an insoluble κ-CRG and protein complex when using pH values above to the IgG pI [4]. The formation of this complex is clearly visible for pH values of 8.0, 9.0 and 10.0 (see Fig. S5 in the Supporting information), and as such these pH values cannot be used to recover IgG. Concerning the IgG purification factor, the best value of 2.7 was obtained at pH 7.0, a similar value to the one obtained in the adsorption assays (IgG purification factor of 3.0). Overall, at pH 7.0 the best results for the desorption of IgG were attained, with an IgG recovery yield of 74% and a purification factor of 2.7.
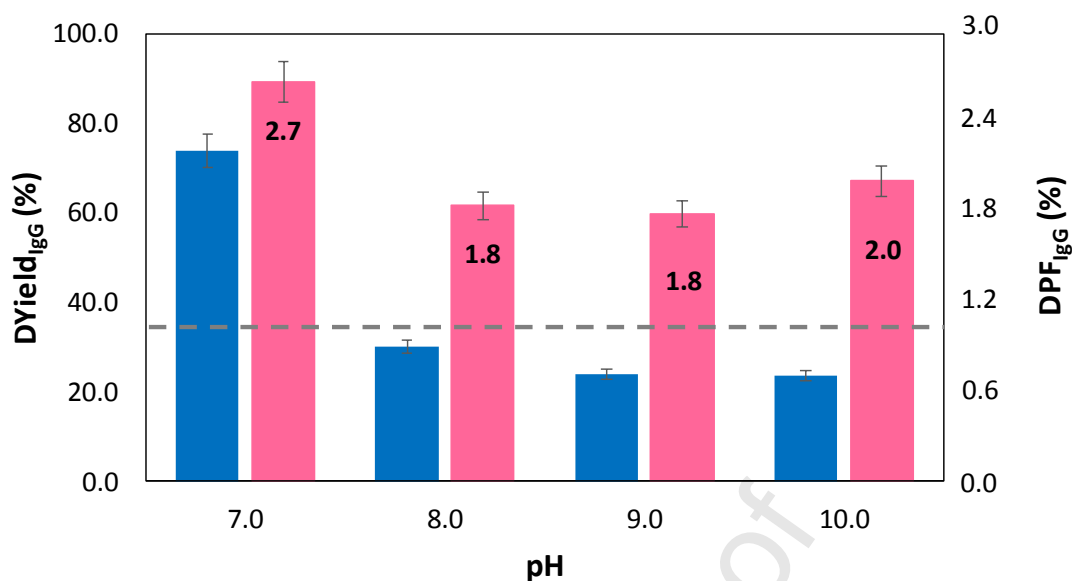
Fig. 6. Recovery yields (%DYield$_{IgG}$ – ■) and purification factors (DPF$_{IgG}$ – ■) of desorbed IgG from HMNP by changing the pH. The dashed line corresponds to the initial IgG purity in the rabbit serum (PF = 1.0). The experiments were performed during 60 min of contact time using 50 mM phosphate (pH 7.0 and 8.0) or carbonate (pH 9.0 and 10.0) buffer.

The evaluation of the IgG and other proteins secondary structure after the adsorption/desorption steps was finally carried out by CD. CD is an appropriate technique for determining the secondary structure of proteins due to the amides present in the polypeptide backbone, that are characteristic of proteins, and which have a chromophoric activity that effectively shifts or splits light into multiple transitions [36]. Because proteins CD spectra are dependent on their conformation, this technique can be used to monitor and evaluate conformational changes due to binding interactions [37]. Fig. S6 in the Supporting Information shows the CD results for the IgG and other proteins after the desorption step with the buffered aqueous solution at pH 7 or KCl solution at 0.5 M. In both spectra it is shown that IgG and other proteins do not present

a significant loss of secondary structure, as shown by their spectrum resemblance with the rabbit serum, with a negative band appearing at 218 nm characteristic of proteins mainly comprising β-sheets [38].

4. Conclusions

Hybrid magnetic nanoparticles comprising a magnetic core of Fe_3O_4 encapsulated with a siliceous shell enriched in the polysaccharide κ-carrageenan are promising novel materials for the adsorption and further purification of IgG. Under the optimized adsorption conditions, IgG with a purification factor three times higher than that in the rabbit serum and an adsorption yield of 90% were achieved. Moreover, the desorption of IgG from HMNP was evaluated, obtaining an IgG purification factor of 2.7 and a recovery yield of 74%. Finally, the maintenance of the secondary structure of IgG after the adsorption and desorption steps was evaluated, confirming the success of the process developed. Overall, the application of HMNPs in the purification of IgG seems to have high potential as a new downstream platform for biologically active biomolecules.

References

[1]   P. Agrawal, Biopharmaceuticals: An emerging trend in drug development, Pharm Pharm Sci. 2 (2015) 1–2. http://dx.doi.org/10.15226/2374-6866/2/1/00120.

[2]   P.A.J. Rosa, I.F. Ferreira, A.M. Azevedo, M.R. Aires-Barros, Aqueous two-phase systems: A viable platform in the manufacturing of biopharmaceuticals., J. Chromatogr. A. 1217 (2010) 2296–2305. https://doi.org/10.1016/j.chroma.2009.11.034.

[3]   D. Mondal, M. Sharma, M.V. Quental, A.P.M. Tavares, K. Prasad, M.G. Freire, Suitability of bio-based ionic liquids for the extraction and purification of IgG antibodies, Green Chem. 18 (2016) 6071–6081. https://doi.org/10.1039/C6GC01482H.

[4]   A.M. Ferreira, V.F.M. Faustino, D. Mondal, J.A.P. Coutinho, M.G. Freire, Improving the extraction and purification of immunoglobulin G by the use of ionic liquids as adjuvants in aqueous biphasic systems, J. Biotechnol. 236 (2016) 166–175. https://doi.org/10.1016/j.jbiotec.2016.08.015.

[5]   A.M. Azevedo, P.A.J. Rosa, I.F. Ferreira, M.R. Aires-Barros, Optimisation of aqueous two-phase extraction of human antibodies., J. Biotechnol. 132 (2007) 209–217. https://doi.org/10.1016/j.jbiotec.2007.04.002.

[6]   C.C. Ramalho, C.M.S.S. Neves, M.V. Quental, J.A.P. Coutinho, M.G. Freire, Separation of immunoglobulin G using aqueous biphasic systems composed of cholinium-based ionic liquids and poly(propylene glycol)., J. Chem. Technol. Biotechnol. 93 (2018) 1931–1939. https://doi.org/10.1002/jctb.5594.

[7]   N. Bereli, A. Denizli, Superior magnetic monodisperse particles for direct purification of immunoglobulin G under magnetic field, J. Macromol. Sci. Part A. 53 (2016) 160–168. https://doi.org/10.1080/10601325.2015.1132914.

[8]   X. Hou, C. Zhao, Y. Tian, S. Dou, X. Zhang, J. Zhao, Preparation of functionalized Fe3O4@SiO2 magnetic nanoparticles for monoclonal antibody purification, Chem. Res. Chinese Univ. 32 (2016) 889–894. https://doi.org/10.1007/s40242-016-6251-y.

[9]   V.L. Dhadge, A. Hussain, A.M. Azevedo, R. Aires-Barros, A.C.A. Roque, Boronic acid-modified magnetic materials for antibody purification., J. R. Soc. Interface. 11 (2014) 20130875. https://doi.org/10.1098/rsif.2013.0875.

[10]   N. Ozturk, M.E. Gunay, S. Akgol, A. Denizli, Silane-modified magnetic beads: application to immunoglobulin G separation., Biotechnol. Prog. 23 (2007) 1149–1156. https://doi.org/10.1021/bp070158o.

[11]   K. Salimi, D.D. Usta, İ. Koçer, E. Çelik, A. Tuncel, Protein A and protein A/G coupled magnetic SiO2 microspheres for affinity purification of immunoglobulin G, Int. J. Biol. Macromol.   111   (2018)   178–185. https://doi.org/https://doi.org/10.1016/j.ijbiomac.2018.01.019.

[12]   S. Sun, Y. Tang, Q. Fu, X. Liu, L. Guo, Y. Zhao, C. Chang, Monolithic cryogels made of agarose–chitosan composite and loaded with agarose beads for purification of immunoglobulin   G,   Int.   J.   Biol.   Macromol.   50   (2012)   1002–1007. https://doi.org/https://doi.org/10.1016/j.ijbiomac.2012.02.028.

[13]   M. Cao, Z. Li, J. Wang, W. Ge, T. Yue, R. Li, V.L. Colvin, W.W. Yu, Food related applications of magnetic iron oxide nanoparticles: Enzyme immobilization, protein purification, and food analysis, Trends Food Sci. Technol. 27 (2012) 47–56. https://doi.org/https://doi.org/10.1016/j.tifs.2012.04.003.

[14]   A.K. Gupta, M. Gupta, Synthesis and surface engineering of iron oxide nanoparticles for biomedical   applications,   Biomaterials.   26   (2005)   3995–4021. https://doi.org/https://doi.org/10.1016/j.biomaterials.2004.10.012.

[15]   G. Aygar, M. Kaya, N. Özkan, S. Kocabıyık, M. Volkan, Preparation of silica coated cobalt ferrite magnetic nanoparticles for the purification of histidine-tagged proteins, J. Phys.   Chem.   Solids.   87   (2015)   64–71. https://doi.org/https://doi.org/10.1016/j.jpcs.2015.08.005.

[16]   S.Z. Mirahmadi-Zare, A. Allafchian, F. Aboutalebi, P. Shojaei, Y. Khazaie, K. Dormiani, L. Lachinani, M.-H. Nasr-Esfahani, Super magnetic nanoparticles $NiFe_2O_4$, coated with aluminum-nickel oxide sol-gel lattices to safe, sensitive and selective purification of his-tagged proteins., Protein Expr. Purif. 121 (2016) 52–60. https://doi.org/10.1016/j.pep.2016.01.008.

[17]   H. Qian, Z. Lin, H. Xu, M. Chen, The efficient and specific isolation of the antibodies from human serum by thiophilic paramagnetic polymer nanospheres, Biotechnol. Prog. 25 (2009) 376–383. https://doi.org/10.1002/btpr.105.

[18]   S.F. Soares, T.R. Simões, M. António, T. Trindade, A.L. Daniel-da-Silva, Hybrid nanoadsorbents for the magnetically assisted removal of metoprolol from water, Chem. Eng. J. 302 (2016) 560–569. https://doi.org/https://doi.org/10.1016/j.cej.2016.05.079.

[19]   Y.P. He, S.Q. Wang, C.R. Li, Y.M. Miao, Z.Y. Wu, B.S. Zou, Synthesis and characterization of functionalized silica-coated Fe_3O_4 superparamagnetic nanocrystals for biological applications, J. Phys. D. Appl. Phys. 38 (2005) 1342–1350. https://doi:10.1088/0022-3727/38/9/003.

[20]   M.A. Martins, T. Trindade, Os Nanomateriais e a Descoberta de Novos Mundos na Bancada do Químico, Quim. Nov. 35 (2012) 1434–1446. http://dx.doi.org/10.1590/S0100-40422012000700026.

[21]   C.- L Wu, Q.- H. Chen, X.- Y. Li, J.-h. Su, S. He, J. Liu, Y. Yuan, Formation and characterisation of food protein–polysaccharide thermal complex particles: effects of pH, temperature and polysaccharide type, Int. J. Food Sci. Technol. (2019) 1–7. https://doi.org/doi:10.1111/ijfs.14416.

[22]   S.V. Patwardhan, G. Patwardhan, C.C. Perry, Interactions of biomolecules with inorganic materials: principles, applications and future prospects, J. Mater. Chem. 17 (2007) 2875–2884. https://doi.org/10.1039/B704075J.

[23]   S.F. Soares, T. Trindade, A.L. Daniel-da-Silva, Carrageenan–Silica Hybrid Nanoparticles Prepared by aNon-Emulsion Method, Eur. J. Inorg. Chem. (2015) 4588–4594. https://doi.org/10.1002/ejic.201500450.

28

[24] K.M. Zia, S. Tabasum, M. Nasif, N. Sultan, N. Aslam, A. Noreen, M. Zuber, A review on synthesis, properties and applications of natural polymer based carrageenan blends and composites, Int. J. Biol. Macromol. 96 (2017) 282–301. https://doi.org/https://doi.org/10.1016/j.ijbiomac.2016.11.095.

[25] S.F. Soares, M.J. Rocha, M. Ferro, C.O. Amorim, J.S. Amaral, T. Trindade, A.L. Daniel-da-Silva, Magnetic nanosorbents with siliceous hybrid shells of alginic acid and carrageenan for removal of ciprofloxacin, Int. J. Biol. Macromol. 139 (2019) 827–841. https://doi.org/https://doi.org/10.1016/j.ijbiomac.2019.08.030.

[26] R. Oliveira-Silva, J. Pinto da Costa, R. Vitorino, A.L. Daniel-da-Silva, Magnetic chelating nanoprobes for enrichment and selective recovery of metalloproteases from human saliva, J. Mater. Chem. B. 3 (2015) 238–249. https://doi.org/10.1039/C4TB01189A.

[27] R. Ortega-Zempoalteca, Y. Flores, G. Vázquez.Victorio, T. Gaudisson, S. Merah, Z. Vargas, U. Acevedo Salas, R. Valenzuela, The effects of spark plasma sintering consolidation on the ferromagnetic resonance spectra (FMR) of Ni–Zn ferrites, Phys. Status Solidi. 211 (2014). https://doi.org/10.1002/pssa.201300762.

[28] Joint Committee for Powder Diffraction Studies (JCPDS), card no. 1 (2002) 0629.

[29] E.P. O'Brien, B.R. Brooks, D. Thirumalai, Effects of pH on proteins: Predictions for ensemble and single-molecule pulling experiments, J. Am. Chem. Soc. 134 (2012) 979–987. https://doi.org/10.1021/ja206557y.

[30] Serum albumin precursor Oryctolagus cuniculus (Rabbit)., SIB Swiss Inst. Bioinforma.

[31] A.K. Stone, M.T. Nickerson, Food Hydrocolloids Formation and functionality of whey protein isolate-(kappa-, iota-, and lambda-type) carrageenan electrostatic complexes, Food Hydrocoll. 27 (2012) 271–277. https://doi.org/10.1016/j.foodhyd.2011.08.006.

[32] S.K. Samant, R.S. Singhal, P.R. Kulkarni, D.V. Rege, Protein-polysaccharide interactions : a new approach in food formulations, Int. J. Food Sci. Technol. 28 (1993) 547–562. https://doi.org/10.1111/j.1365-2621.1993.tb01306.x.

[33] A. Tecante, M. Santiago, solution properties of κ-carrageenan and its interaction with

29

other polysaccharides in aqueous media, in: J. Vicente (Ed.), Rheology, IntechOpen, 2012. https://doi.org/10.5772/36619.

[34] C.H. Lochmüller, L.S. Wigman, B.S. Kitchell, Aerosol- jet produced, magnetic carrageenan- gel particles: A new affinity chromatography matrix, Technol. Biotechnol. 40 (1987) 33–40. https://doi.org/10.1002/jctb.280400104.

[35] T.H.M. Snoeren, C.A.Van Der Spek, T.A.J. Payens, Preparation of κ-and minor αs-casein by electrostatic affinity chromatography, Biochim. Biophys. Acta (BBA)-Protein Struct. 490 (1977) 255–259. https://doi.org/10.1016/0005-2795(77)90127-1.

[36] K.D. Philipson, K. Sauer, Exciton interaction in a bacteriochlorophyll-protein from Chloropseudomonas ethylicum. Absorption and circular dichroism at 77°K, Biochemistry. 11 (1972) 1880–1885. https://doi.org/10.1021/bi00760a024.

[37] F.H. Niesen, H. Berglund, M. Vedadi, The use of differential scanning fluorimetry to detect ligand interactions that promote protein stability., Nat. Protoc. 2 (2007) 2212–2221. https://doi.org/10.1038/nprot.2007.321.

[38] M. Shimizu, H. Nagashima, K. Sano, K. Hashimoto, M. Ozeki, K. Tsuda, H. Hatta, Molecular stability of chicken and rabbit immunoglobulin G, Biosci. Biotechnol. Biochem. 56 (1992) 270–274. https://doi.org/10.1271/bbb.56.270.

30

Author statement

Magalhães, Flávia F. Investigation; Formal analysis

Almeida, Mafalda R. Formal analysis; Validation; Roles/Writing–original draft

Soares, Sofia F. Investigation; Formal analysis.

Trindade, Tito Funding acquisition; Resources; Methodology; Writing – review & editing

Freire, Mara G. Funding acquisition; Resources; Methodology; Writing – review & editing

Daniel-da-Silva, Ana Luísa Conceptualization; Funding acquisition; Methodology; Resources; Supervision; Writing – review & editing

Tavares, Ana P. M. Conceptualization; Methodology; Project administration; Supervision; Writing – review & editing

Graphical abstract

Highlights:

- A simple method for the IgG adsorption and purification from rabbit serum was developed

- A high IgG purification factor was achieved with siliceous-polysaccharide hybrid magnetic nanoparticles

- IgG is effectively recovered from the magnetic nanoparticles using buffered aqueous solutions